Available online at www.sciencedirect.com
SCIENCE DIRECT
International Journal of Heat and Mass Transfer 49 (2006) 1015–1021
International Journal of HEAT and MASS TRANSFER
www.elsevier.com/locate/ijhmt

"3D layered thermography" method to map the temperature distribution of a free flowing bulk in case of microwave drying

Akos Kelen [a,*], Sandor Ress [b], Tibor Nagy [a], Erzsebet Pallai-Varsanyi [c], Klara Pintye-Hodi [d]

[a] Formulation Development, Richter Gedeon Ltd., Budapest 10, P.O. Box 27, Budapest H-1475, Hungary
[b] Department of Electron Devices, Technical University of Budapest, Muegyetem rkp 3, Budapest H-1521, Hungary
[c] Research Institute of Chemical and Process Engineering, University of Veszprem, Egyetem u. 2, Veszprem H-8200, Hungary
[d] Department of Pharmaceutical Technology, University of Szeged, Eotvos u. 6, Szeged H-6720, Hungary

Received 25 March 2005; received in revised form 14 September 2005
Available online 22 November 2005

Abstract

Microwave drying is getting more and more popular even in the highly regulated pharmaceutical field. In spite of its uniqueness there is a rightful resistance because of the non-homogeneous electric field that cause non-homogeneous temperature distribution. The dielectric and thermal properties of any complex workload are rarely known, and moreover, they change during a drying process, which makes experimental tests essential to complete any mathematical modelling. To get a 3D overview of a free-flowing bulk the workload was divided with Teflon layers to form cross-sectional surfaces. After dissipation of microwave energy, IR thermocartograms were taken and temperature distribution was evaluated even quantitatively. The "3D layered thermography" method offers reliable and workload-specific information via simple executable technique for the optimization of a microwave processes.

Keywords: Microwave; Homogeneity; Heat sensitive; Hot spot; Thermography

1. Introduction

The benefits and drawbacks of microwave drying in the conservative pharmaceutical industry have been well known for decades. In spite of the fact that dielectric drying offers unique advantages [1] the biggest resistance to widespread use may be the confirmed non-uniformity of the electromagnetic field (E-field), which results in a non-homogeneous temperature pattern [2,3]. The origin and result of a generated hot-spot is influenced by the electromagnetic and thermodynamic features of the microwave system and the workload. Hotter areas are cooled by heat diffusion to the surrounding material, determined by the thermal diffusivity and the temperature gradient. The use of microwaves can be risky if the workload's thermal diffusivity is low, in which case the heat flow is slower than the rate of energy dissipation.

When a drying of extremely fragile corn starch-based granules was carried out in vacuum and accelerated by microwaves in single/one pot equipment (a double-jacketed high-shear granulator that incorporates vacuum and microwave drying options), local burning was experienced after 25 min of microwave heating. The local "hot spot" temperature of the product must have been over 200 °C because of the carbonization (Fig. 1). At the same time the measured temperature of the surrounding "spot-related" product was just around 50–60 °C (Fig. 2). The browning could not be noticed by the monochrome CCD video system, because this area of the workload was located out of its visual field (Fig. 3).

In case of single/one pot technology the geometry and the construction of the microwave cavity is primarily

* Corresponding author. Tel.: +36 1 431 5675; fax: +36 1 431 5979.
E-mail address: a.kelen@richter.hu (A. Kelen).

0017-9310/$ - see front matter © 2005 Elsevier Ltd. All rights reserved.
doi:10.1016/j.ijheatmasstransfer.2005.09.006

Nomenclature

A	comprises the different attenuations and losses
$A_{n_x i_y}$	by the IR camera-measured surface
c_{xx}	specific heat capacity of the indicated material
$d_{n_x} = d$	thickness
E_d	dissipated microwave energy
E_i	electric-field strength within the dielectric
f	microwave frequency
i_y	temperature range ($i_{25–30}, \ldots, i_{95–100}$)
L_v	heat of vaporization
M	mass of the whole workload
$M^*_{i_y}$	percent of the total material mass characterized by an i_y temperature range (%)
m_{n_x}; $m_{n_x i_y}$; m_{xx}	mass of the indicated material or part (kg)
$m^*_{n_x i_y}$	percent of the material mass characterized by an i_y temperature range wit hin the n_x layer (%)
n_x	layer ($n_1, \ldots, n_6$)
P_d	dissipated microwave power
P_m	magnetron output power
P_r	the reflected power
Q	quantity of heat
$Q_{xx(t_{yy} \to t_{zz})}$	quantity of heat of the indicated material in the given temperature range
U	internal energy
t	time
$\overline{T}_{i_y}$	mean temperature of the incidental i_y temperature range
$\overline{T}_{n_x}$	average temperature of the n_x layer
W	work
W_evap	evaporation work
W_volum	volumetric work

Greek symbols

ε_0	absolute permittivity
ε	loss factor of the dielectric material
$\Delta T_{(t_{yy} \to t_{zz})}$	temperature difference between the indexed events
$\rho_{n_x} = \rho$	density of the workload

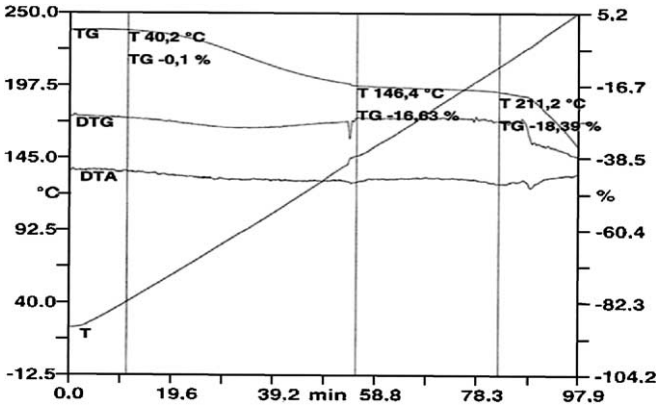

Fig. 1. TG curve of corn starch.

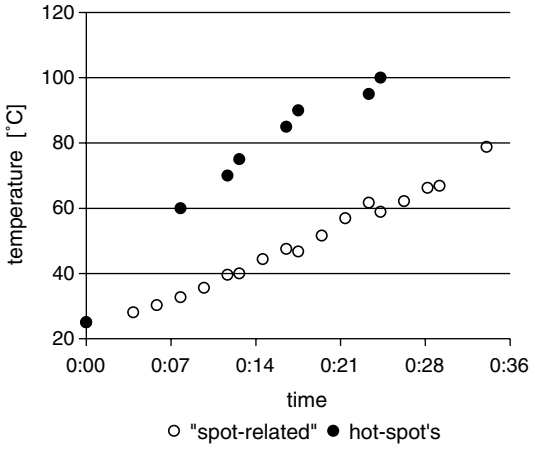

Fig. 2. Temperature–time curve of corn starch. "Spot-related" is measured during the running process, hot-spot's immediately after microwaves was switched off (6.3 kg, 50 mbar, 1.2 kW, 2450 MHz), $n = 3$.

designed for high-sheer granulation, thus to avoid the undesirable unequal temperature distribution there are limited possible solutions, e.g. the intensification of the mixer motion, and/or the reduction of the microwave power. The former would change the grain-size distribution unacceptably, while the latter would considerably increase the process time. As a result of experimental process optimization the best uniformity and acceptable highest power density, as well as the shortest drying time are sought, without any corresponding damage of the workload, thus the process is close to its secure limit.

The aim of the present study is to specify this limit and for that very reason to map the forming stereoscopic temperature pattern in the case of a free-flowing bulk workload (e.g. powder, granule, grain crops, etc.). In this paper we do not focus on the microscopic details [4,5] rather just on its macroscopic result.

2. Theoretical aspects

2.1. Non-homogeneity of microwaves

Field concentration of standing waves or close proximity to the power-feed-point can cause non-uniform distribution of the microwave field [6]. Many factors influence the uniformity of the E-field. They can be divided roughly into two groups: cavity effects (design limitation, location of the microwave inlet point, shape of the cavity, hanging

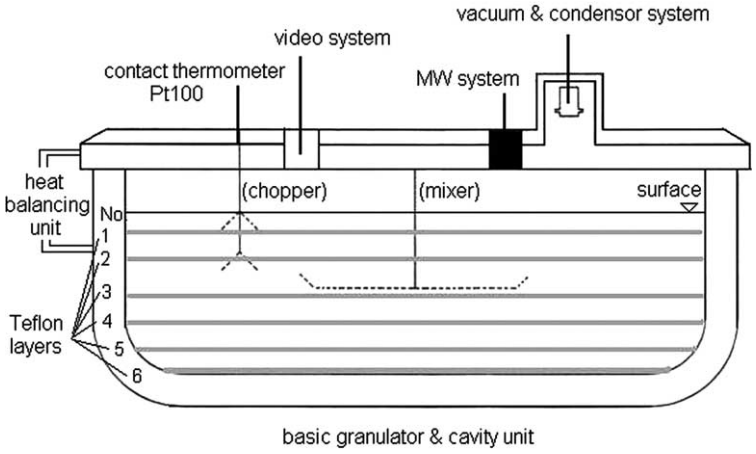

Fig. 3. Single/one pot apparatus equipped with Teflon layers.

parts such as spray gun, mixer, chopper, thermometer etc.) and workload interactions (loss factor, penetration depth and thickness of the workload, particle's feature, etc.) that are different from product to product and from equipment to equipment.

Inter alia "mechanical moving mode stirrers" or "waveguide rotating joints" or simple agitation of the workload are used to assure more uniform E-field distribution, and thus heating. Adequate homogeneity can be achieved e.g. in a developed microwave applicator, characterised by cylindrical shape and adjusted with several magnetrons [7]. In the case of special single/one pot pharmaceutical microwave equipment the number and place of magnetrons are very limited due to its primary functional purpose, thus agitation of the workload is preferred that may endanger the quality of the product.

2.2. Theoretical models

An inherent deficiency of dielectric drying is that there is no common method to control, nor to properly monitor the E-field distribution and its effect after starting the microwave treatment. With the help of mathematical models based on Maxwell's equations the theoretical electric and magnetic field configuration within the product can be calculated [8,9] even in 3D [10,11], if the configuration of the cavity, the dielectric properties of the workload and the granule's geometry, etc. are exactly known. The following dielectric heating equation is also used to calculate the dissipated microwave power (P_d) [3,9]:

$$P_d = 2\pi f \varepsilon_0 \varepsilon'' E_i^2 \tag{1}$$

The calculations involve difficulties especially in the case of complex compositions (e.g. pharmaceutical and food products). The workload consists of several ingredients characterised by different and often unknown dielectric and thermal properties that are furthermore changing continuously during the drying process depending on the changing moisture content and temperature. Moreover the temperature and the moisture content dependencies of the dielectric characteristics are also rarely known. For that reason, experimental tests can never be omitted.

The internal energy (U) of the product being dried in microwave oven changes by the absorbed (dissipated) microwave energy (E_d). Based on the first law of thermodynamics, temperature is considered as an indicator of E-field. The change of the internal energy can be expressed by the following relations:

$$\Delta U = \Sigma Q - \Sigma W \tag{2}$$

$$\Delta U = Q_{\text{solvent}(t_{\text{start}} \to t_{\text{BP}})} + Q_{\text{steam}_{(t_{\text{BP}} \to t_{\text{end}})}} + Q_{\text{solid}(t_{\text{start}} \to t_{\text{end}})} - W_{\text{volum}} + W_{\text{evap}} \tag{3}$$

$$\Delta U = c_{\text{solvent}} m_{\text{solvent}} \Delta T_{(t_{\text{start}} \to t_{\text{BP}})} + c_{\text{steam}} m_{\text{steam}} \Delta T_{(t_{\text{BP}} \to t_{\text{end}})} + c_{\text{solid}} m_{\text{solid}} \Delta T_{(t_{\text{start}} \to t_{\text{end}})} - p\Delta V + L_v m_{\text{solvent}} \tag{4}$$

The energy dissipation of the steam which is actually present in the cavity is negligible due to its small amount ($m_{\text{steam}} \approx 1$ g). There is no volumetric work ($\Delta V \approx 0$).

$$\Delta U = c_{\text{solvent}} m_{\text{solvent}} \Delta T_{(t_{\text{start}} \to t_{\text{BP}})} + c_{\text{solid}} m_{\text{solid}} \Delta T_{(t_{\text{start}} \to t_{\text{end}})} + L_v m_{\text{solvent}} \tag{5}$$

In accordance with the presented it can be stated that the change of the temperature is proportional to the change of the internal energy. The change of the internal energy during microwave drying can be calculated on the basis of the dissipated microwave power (P_d) and the microwave treatment time (t).

$$\Delta U = E_d = P_d t \tag{6}$$

For experimental determination of the dissipated microwave power a special instrumental set-up is required fit to measure the magnetron output power (P_m), the reflected power (P_r) and all the losses that are evolved in the set-up (e.g. losses by the direction coupling, by fitting attenuation, etc.). Based on the measured reflected microwave power, the dissipated microwave power can be calculated by the following equation [12]:

$$P_d = P_m - AP_r \tag{7}$$

3. Experimental techniques

3.1. Experimental methods for determination of the temperature (microwave energy) distribution in microwave treated workload

In the case of dielectric heating without any mixing motions the location and the temperature of hot spots are a mystery, thus to obtain information on these values is very limited from the energy distribution point of view [13].

3.1.1. Thermography

Among the neither perturbing, nor intrusive temperature-monitoring alternatives, infrared imaging is known as one of the most promising. The unique advantage of IR monitoring is that it does not disturb the drying at all and a huge quantity of data can be recorded digitally and displayed instantly [14]. The limitation of IR monitoring is that it provides information exclusively about the monitored surface. Ohlsson et al. made cross sections of solid objects and used thermal imaging to get 3D information about their temperature distributions [15].

3.1.2. Mapping the temperature distribution in 3D

Vass and Pallai elaborated a method to map the 3D temperature distribution in microwave heated granular workload [16]. Special foils with given softening temperature were placed into the workload on the surface of different layer-levels. By microwave heating the granules of the workload stick into those areas of the foils at or above the softening temperature and form a so called 3D heatmap. Using foils with different softening temperatures also the exact temperatures could be determined. Quite a number of trials are needed to map the whole workload.

3.1.2.1. The elaborated "3D layered thermography" mapping method. In our experiments the workload is corn starch (Roquette GmbH, Germany) as a common pharmaceutical diluent. Teflon (PTFE) disks of 1 cm thickness are used to divide the workload horizontally into six corn starch layers of 2 cm thickness. Between the layers tiny Teflon distance pieces assure the even density of corn starch, because it is known that the loss factors of granular materials are dependent on bulk density [17]. The change of the dielectric and thermal properties of the starch depend on its moisture content. During the drying process the moisture content changed from 13% to a value close to zero, while the temperature increased from 25 °C to 100 °C. In this particular case, these differences were neglected due to the minimal change of thermodynamic features [18] and dielectric properties [19].

The workload (6.3 kg, 2/3 of the total capacity) was divided by Teflon disks and heated by microwaves at 1.2 kW (2450 MHz) under pressure of 50 ± 5 mbar in a single pot system (Fig. 3) (Collette Ultima 25 l, Collette NV, Belgium). At first the temperature of the double-jacket of

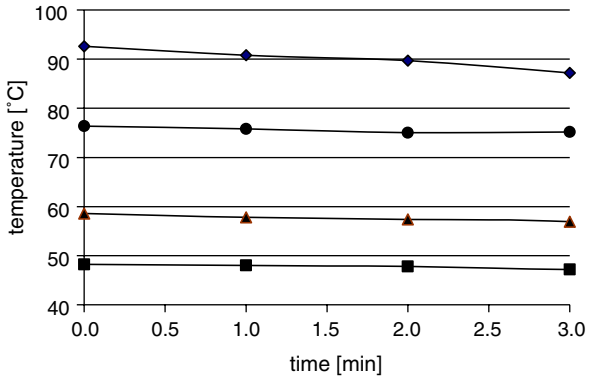

Fig. 4. Transient temperature of corn starch at different initial temperatures (the long-wave emission constant of corn starch is 0.95).

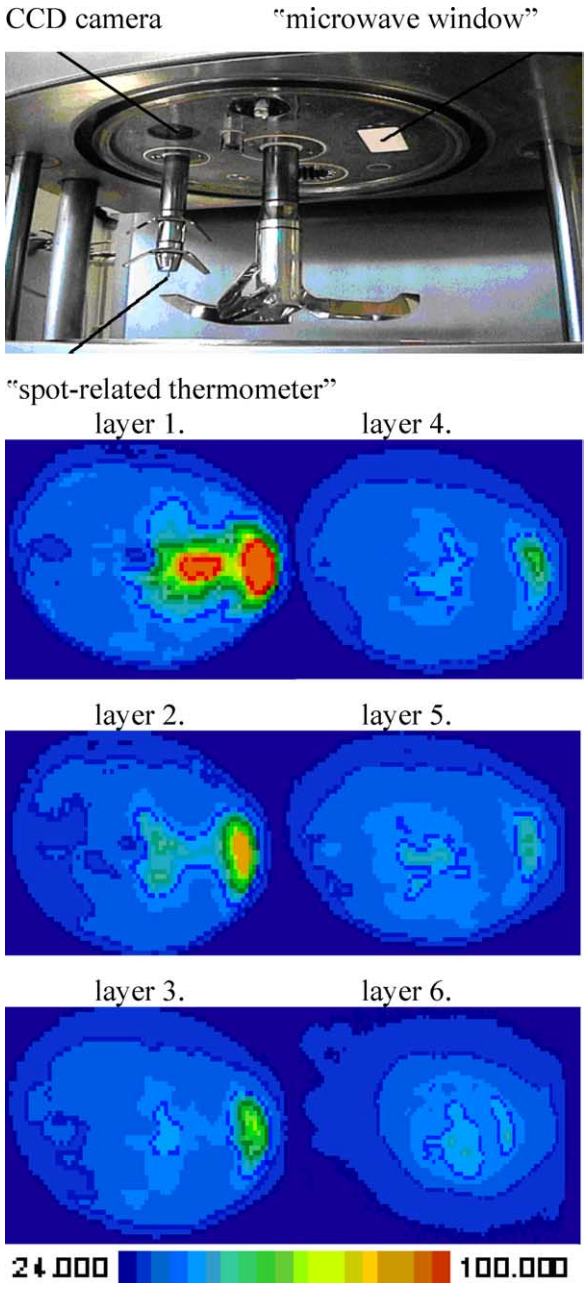

Fig. 5. The lid of the equipment and 2D thermocartograms of the layers.

the cavity and the workload were tempered at 25 °C for 60 min. The temperature of the condenser was controlled at 6 ± 1 °C during the drying processes. The circulation in the cooling system was blocked, thus the double-jacket was heated up exclusively by thermal conduction. After a given drying time (25 min) all the six corn starch layers were immediately monitored one by one by infrared camera (AGA782 Infrared Imaging System, Infrared System AB, Sweden). The sensitivity of the temperature determination was 0.2 °C. All the six snapshots were taken within 1 min after the microwave was switched off. Transient IR snapshots [20] prove that the temperature decrease between the end of the microwave treatment and taking the thermograms is negligible (Fig. 4).

4. Results and discussion

Thermal imaging offers immediate 2D visual information. It is easy to evaluate the coloured temperature distribution patterns of each layer (Fig. 5) according to the required temperature ranges. (In the pharmaceutical technology a temperature range of ±5 °C is yet acceptable). In the case of dielectric drying of corn starch, the hottest area is situated directly under the microwave inlet window. Based on preliminary tests the vertical temperature difference within the corn starch layers of 2 cm thickness was never greater than 1–2 °C, thus the temperature of the whole amount under a given surface can be characterised by the surface temperature.

The obtained thermocartograms were evaluated to produce a certain 3D pattern of temperature as well as of E-field distribution in the workload. Due to this ''layered thermography'' technique, the temperature and its distribution can be identified even quantitatively according to the following method (Table 1 and Fig. 6).

The mass ($m_{n_x i_y}$/ kg) of a bulk characterised by a chosen temperature range ($i_y : i_{25–30}, \ldots, i_{95–100}$) in a layer ($n_x : n_1, \ldots, n_6$) can be calculated by the camera-measured surface ($A_{n_x i_y}/m^2$), the known thickness ($d_{n_x} = d =$ constant/m) and the density ($\rho_{n_x} = \rho =$ constant/kg/m^3) of the product layer.

$$m_{n_x i_y} = A_{n_x i_y} d\rho \tag{8}$$

The percent of the material mass ($m^*_{n_x i_y}$/%) characterized by an i_y temperature range within the n_x layer can be calculated with the help of the given mass in question ($m_{n_x i_y}$/kg) and the known mass of the entire layer (m_{n_x}/kg)

$$m^*_{n_x i_y} = \frac{m_{n_x i_y}}{m_{n_x}} \cdot 100 \tag{9}$$

The percent of the total material mass ($M^*_{i_y}$/%) characterized by an i_y temperature range within the whole workload (M/kg) is

$$M^*_{i_y} = \frac{M_{i_y}}{M} \cdot 100 \tag{10}$$

The average temperature of the n_x layer ($\overline{T}_{n_x}$/°C) can be calculated by the percent of the material characterized by an i_y temperature range within the n_x layer ($m^*_{n_x i_y}$/%) weighted by the mean temperature of the incidental i_y temperature range ($\overline{T}_{i_y}$/°C).

$$\overline{T}_{n_x} = \Sigma(m^*_{n_x i_y} \cdot \overline{T}_{i_y})/100 \tag{11}$$

The presented ''3D layered thermography'' technique offers even quantitative information about temperature distribution of a free-flowing workload in a simple way. It is

Table 1
The quantitative and qualitative evaluation of the temperature distribution based on ''layered thermography''

T_{i_y} (°C)	Layer no. (n_x)						$M^*_{i_y}$ (%)
	1 $m^*_{n_x} i_y$ (%)	2 $m^*_{n_x} i_y$ (%)	3 $m^*_{n_x} i_y$ (%)	4 $m^*_{n_x} i_y$ (%)	5 $m^*_{n_x} i_y$ (%)	6 $m^*_{n_x} i_y$ (%)	
20–25	16.3	3.2	–	–	–	–	3.2
25–30	21.9	33.9	37.3	34.9	31.3	13.9	28.9
30–35	19.9	39.1	39.1	37.7	34.9	39.1	34.9
35–40	20.7	10.5	18.0	20.7	26.4	38.3	22.4
40–45	6.1	7.2	3.1	5.0	5.7	8.6	5.9
45–50	3.2	3.5	0.7	1.0	1.8	–	1.7
50–55	2.2	0.7	0.5	0.5	–	–	0.6
55–60	1.6	0.6	0.5	0.2	–	–	0.4
60–65	1.4	0.4	0.6	–	–	–	0.4
65–70	1.2	0.3	0.1	–	–	–	0.2
70–75	1.0	0.2	–	–	–	–	0.2
75–80	0.8	0.2	–	–	–	–	0.2
80–85	0.6	0.2	–	–	–	–	0.1
85–90	0.6	0.4	–	–	–	–	0.2
90–95	0.6	–	–	–	–	–	0.1
95–100	2.1	–	–	–	–	–	0.4
$\overline{T}_{n_x}$ (°C)	36.7	33.2	32.4	32.6	33.1	34.6	33.7

T_{i_y} = temperature range; $M^*_{i_y}$ = percent of the total material in the i_y temperature range within the whole workload; $m^*_{n_x i_y}$ = percent of the material in the i_y temperature range within the n_x layer; $\overline{T}_{n_x}$ = average temperature of the n_x layer; $\overline{T}$ = average temperature of the total workload.

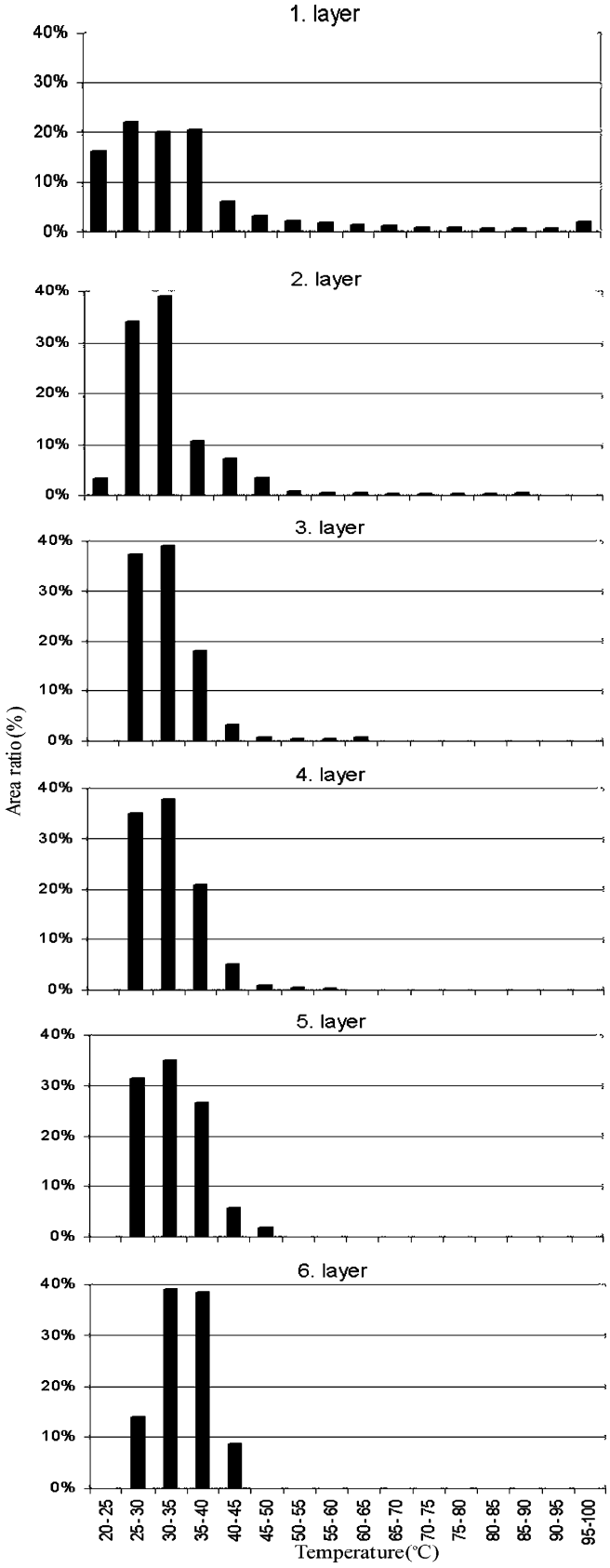

Fig. 6. The different layers are characterized by different temperature distributions, $n = 3$.

not suitable for monitoring directly during a running process, but based on the confirmed reproducibility of E-field distribution, it makes the modelling of a real microwave assisted drying possible even in the case of a pharmaceutical composition characterised by unknown and continuously changing features.

5. Conclusions

Monitoring of temperature distribution in the case of microwave vacuum drying is essential in the pharmaceutical and food industry to prevent even local undesirably high product temperature.

The elaborated "layered thermography" technique provides reliable and quantified 3D information about heat distribution even in the case of a free-flowing bulk. In the case of microwave vacuum drying in a pharmaceutical high-shear granulator the temperature measuring possibility during a running process is very limited due to its functional reason. Add to this that the dielectric and thermal properties of a complex pharmaceutical composition are rarely known, and moreover change during the process, therefore preliminary tests can never be neglected.

The "3D layered thermography" method offers reproducible, reliable and workload-specific information for the drying process optimization.

Acknowledgements

The authors thank Laszlo Csernak, Attila Bodis and Andrasne Kucsera.

References

[1] M.E. Aulton, Radiation drying of wet solid, in: Pharmaceutics, second ed., Churchill Livingstone, London, 2002, pp. 386–388.
[2] A.F. Harvey, Microwave Engineering, Academic Press, New York, 1963.
[3] A.C. Metaxas, R.J. Meredith, Dielectric properties, in: Industrial Microwave Heating, second ed., Peter Peregrinus Ltd., London, 1988, p. 57.
[4] J. Berlan, Microwaves in chemistry another way of heating reaction mixture, Radiat. Phys. Chem. 45 (4) (1995) 581–589.
[5] V.V. Levdansky, H.Y. Kim, H.C. Kim, J. Smolik, P. Moravec, Effect of electromagnetic fields on transfer processes in heterogeneous systems, Int. J. Heat Mass Transfer 44 (2001) 1065–1071.
[6] G. Duschler, W. Carius, K.H. Bauer, Single-step granulation method with microwaves preliminary studies and pilot scale results, Drug Dev. Ind. Pharm. 21 (14) (1995) 1599–1610.
[7] J. Suhm, M. Möller, Aufbau von Mikrowellenanlagen, in: Proceedings of OTTI-Profiforum Mikrowellen-Thermoprozesstechnik Grundlagen, Anlagen und Anwendungen, Deutschland, 2003, CD.
[8] Q. Zhang, T.H. Jackson, A. Ungan, Numerical modelling of microwave induced natural convention, Int. J. Heat Mass Transfer 43 (2000) 2141–2154.
[9] R. Meredith, Introduction and fundamental concepts, in: Engineers' Handbook of Industrial Microwave Heating, The Institution of Electrical Engineers, London, 1998, pp. 7–13, and pp. 21–24.
[10] V.A. Mechenova, V.V. Yakovlev, Efficiency optimization for systems and components in microwave power engineering, J. Microwave Power EE 39 (1) (2004) 15–29.

[11] A. Hallac, A.C. Metaxas, Finite element time domain analysis of microwave heating applicators using higher order vector finite elements, in: Proceedings of 9th International Conference on Microwave and High Frequency Heating, UK, 2003, p. 021.
[12] A. Gollei, L. Ludanyi, E. Pallai, A. Vass, E. Szijjarto, Power engineering study of combined microwave and convective drying, in: Proceedings of 6th International Conference on Food-Science, Hungary, 2004, CD.
[13] W.E. Olmstead, M.E. Brodwin, A model for thermocouple sensitivity during microwave heating, Int. J. Heat Mass Transfer 40 (7) (1997) 1559–1565.
[14] J. Bows, Infrared imaging feels the heat in microwave ovens, Phys. World 5 (1992) 21–22.
[15] T. Ohlsson, P.O. Risman, Temperature distribution of microwave heating spheres and cylinders, J. Microwave Power EE 13 (4) (1987) 303–310.
[16] A. Vass, J. Dudas, J. Csaplaros, E. Pallai, M. Hasznos, Simple and effective method for mapping the microwave field distribution in microwave ovens used for organic synthesis, in: Proceedings of 6th International Conference on Microwave and RF Heating, Italy, 1997, pp. 72–75.
[17] S. Nelson, Density dependence of dielectric properties of particulate materials, Trans. ASAE 26 (1983) 1823–1825.
[18] M.K. Ndife, G. Sumnu, L. Bayindrili, Dielectric properties of six different species of starch at 2450 MHz, Food Res. Int. 31 (1) (1998) 43–52.
[19] C.M. McLoughlin, W.A.M. McMinn, T.R.A. Magee, Physical and dielectric properties of pharmaceutical powders, Power Technol 134 (2003) 40–51.
[20] V. Szekely, S. Ress, A. Poppe, S. Torok, D. Magyari, Zs. Benedek, K. Torki, B. Courtois, M. Rencz, New approaches in the transient thermal measurements, Microelectr. J. 31 (2000) 727–733.